Instrument Science Report WFC3 2002-04

Using global PSF properties to probe the WFC3 UVIS alignment and focus

Massimo Stiavelli,
Christopher Hanley,
August 23, 2001

Abstract

This ISR briefly reviews how the WFC3 UVIS channel focus and alignment impact the PSF. The aim is to verify whether we can identify any simple PSF measurement that would allows to monitor these quantities. We find that the centering of the PSF within a pixel is a crucial parameter that needs to be calibrated or corrected for and that PSF sharpness is the most promising parameter.

1. Introduction

It is customary to check the focus and alignment of HST instruments by carrying out either a full fledged wavefront analysis or a PSF fitting based on a Zernike expansion (see, e.g., Krist and Hook, 1997, Data Analysis Workshop, p. 192). Both techniques can yield accurate results but are somewhat time-consuming. Thus, it would be useful to identify a simpler technique, simply and directly applicable to astronomical images, and able to provide some indications regarding the focus and alignment of the instrument. Such techniques would be applicable both during thermal vacuum testing and ground calibration as well as for routine (possibly automated) monitoring on orbit.

The aim of this ISR is to focus on the WFC3 UVIS channel and investigate whether simple methods based on PSF width, encircled energy and sharpness can provide adequate monitoring of the instrument focus and alignment. The first step is to generate realistic PSFs for the instrument (Section 2). The PSF properties are then measured using automated scripts (Section 3). A discussion of the results can be found in Section 4.

2. Generating realistic PSFs for the WFC3 UVIS channel

In order to compute PSFs for WFC3 UVIS we start out from the optical prescriptions for the channel. Zemax 10.0 is used to compute PSFs at the center of the field of view and for the F631N filter which is the closest to the wavelength used for optical alignment on the ground. The filter is simulated by specifying the filter throughput curve by using a a suitable set of wavelengths and weights in the system wavelengths menu of Zemax. Zemax is the used to compute an ASCII output describing the PSF and its sampling scale. This file is then fed to a Fortran program developed for this project. The Fortran program bins the ideal PSF to the WFC3 UVIS pixel size (0.040") and applies a correction for the Pixel Response Function (PRF). Since the PRF for the WFC3 CCDs has not yet been measured we have adopted the WFPC2 PRF. In a future study we will use either theWFC3 PRF or that measured for ACS/WFC which should be more representative since both WFC3 UVIS and ACS/WFC use thinned, back illuminated CCDs. For each ideal PSF we produce 6 PSFs with different sub-pixel centers and infinite S/N. The results showed in the next section are for the mean of the 6 PSF positions and the errorbar represents the error on the mean. This is provided as an estimate of the measurement accuracy for a realistic situation where a few stars (6-10) are located near the center of the FOV and are used for the measurement. In Figure 1 we show, as an illustration of the method, the ideal PSF and those obtained after pixel sampling both in and out of focus. In this first study we have considered shifts of the secondary mirror of HST and shifts and tilts of the pickoff, and of the M1 and M2 mirrors of WFC3. In order to check the method we compute the PSF also for tilts along the axis perpendicular to the surface (since this should not affect the PSF). Ttilts and displacements considered here are representative of those we would need to measure.

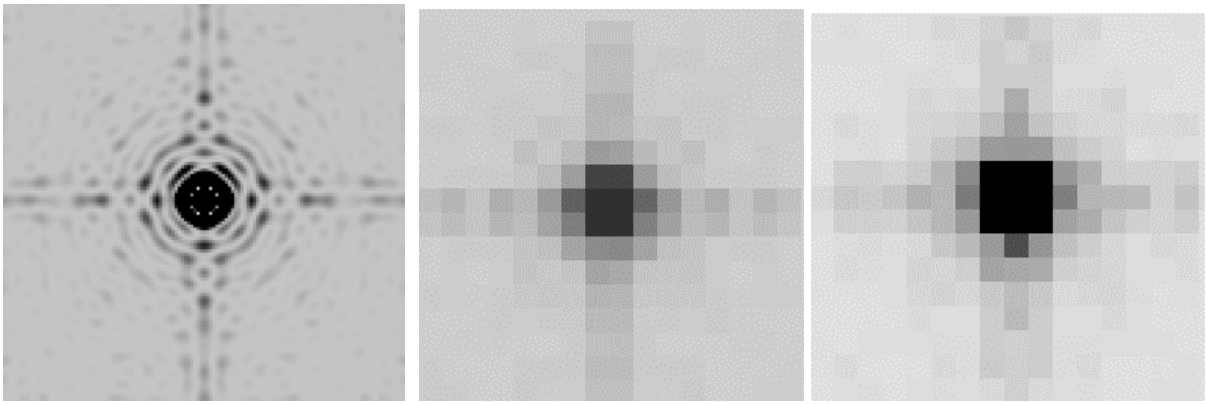

Figure 1: from left to right we show the ideal PSF in the F631N filter (before pixel sampling), the on focus PSF binned to the WFC3 UVIS pixel size, and the PSF at the same location obtained when the secondary mirror of HST is off nominal focus by 9 μm.

3. The global properties of the WFC3 UVIS PSF

We have decided to focus mostly on the PSF FWHM and on the encircled energy within a 3 pixel radius as measured by IRAF/imexam. In addition, the program rebinning the ideal PSF to the final pixels also computes the sharpness of the derived PSF. The sharpness is defined as the sum of the square of the PSF. Its inverse determines the effective number of

pixels contributing to the noise in the photometry of point sources with optimal extraction. Figures 2, 3, 4 and 5 show the variations of encircled energy and FWHM and its uncertainty for displacements of the HST secondary mirror , the pickoff mirror, M1, and M2, respectively.

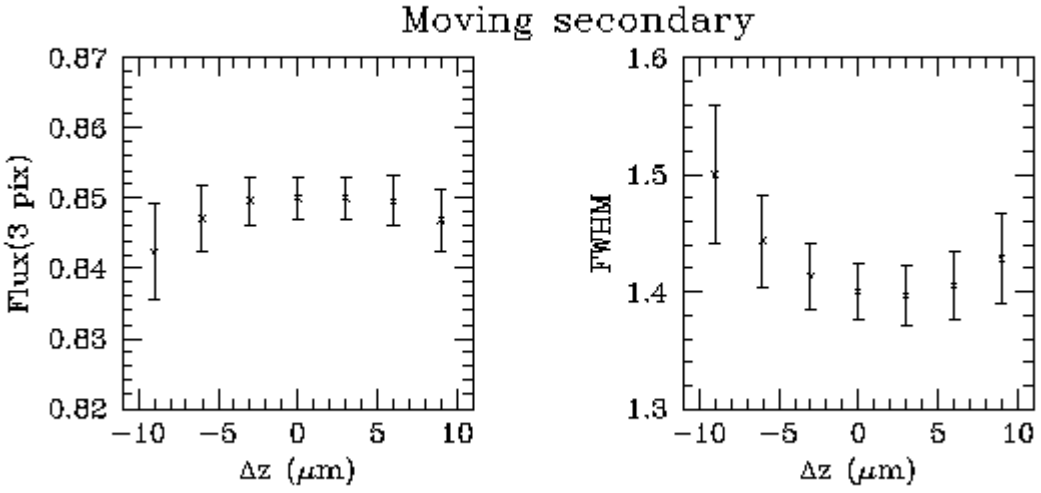

Figure 2 : changes of the encircled energy and FWHM as a function of secondary mirror position. Notice how the error bars representing PSF position uncertainties at the subpixel level are large compared to the effect we intend to measure.

The error bars in the figure represent the measurement uncertainty due to the position of the PSF within a pixel. All these measurements have already been carried on stars centered at 6 different subpixel positions. In order to further reduce the error bar one would need either to calibrate and correct for the effect on a star by star basis or make use of a much larger number of stars. Clearly, for all measurements the encircled energy appears to be the least promising diagnostic. Even for secondary mirror movements it only appears to be sensitive to large displacements (>> 5 microns) and it is essentially insensitive to the displacements of the other surfaces. The FWHM is somewhat better but it still retains many of the limitations discussed above for the encircled energy.

Figures 7, 8, 9, and 10, show similar plots for the PSF sharpness. Comparing, e.g., Figure 2 and Figure 7 shows how the PSF sharpness is much better suited for checking focus and alignment of the instrument. It should be stressed that even when using the sharpness it is important to average the measurement over a few stars in order to reduce the effect due to sub-pixel positioning.

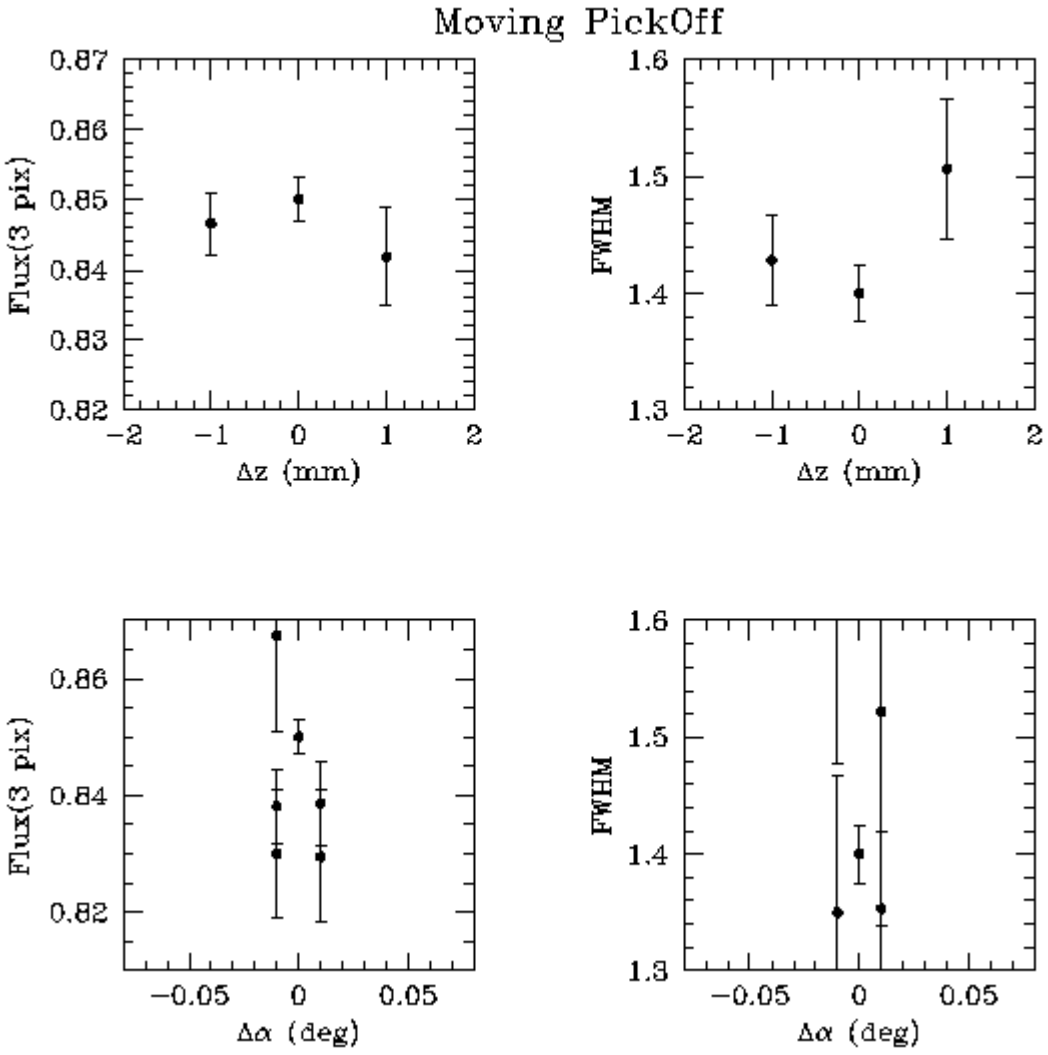

Figure 3 : changes of the encircled energy and FWHM as a function of pickoff position (upper panels) and tilt (lower panels).

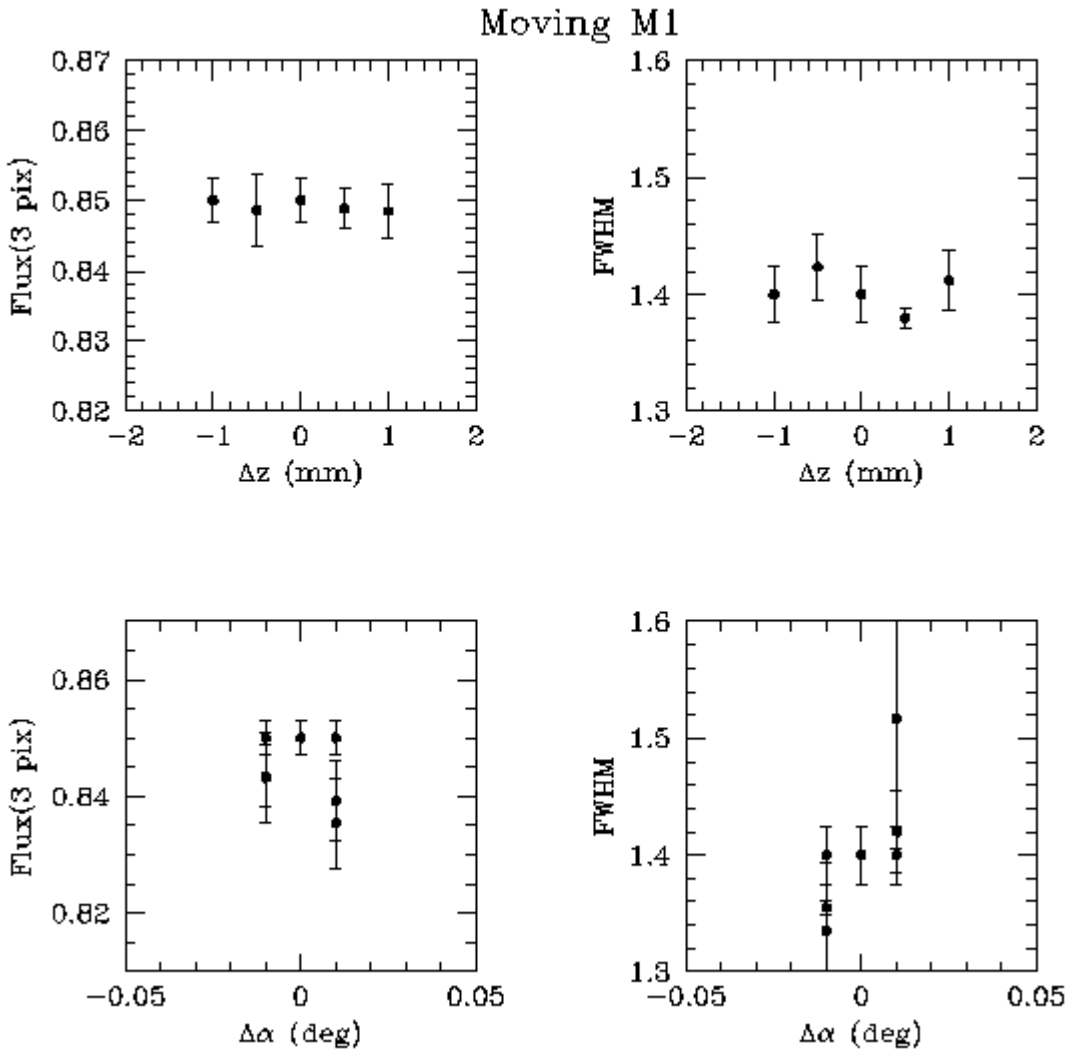

Figure 4 : changes of the encircled energy and FWHM as a function of the M1 mirror position (upper panels) and tilt (lower panels).

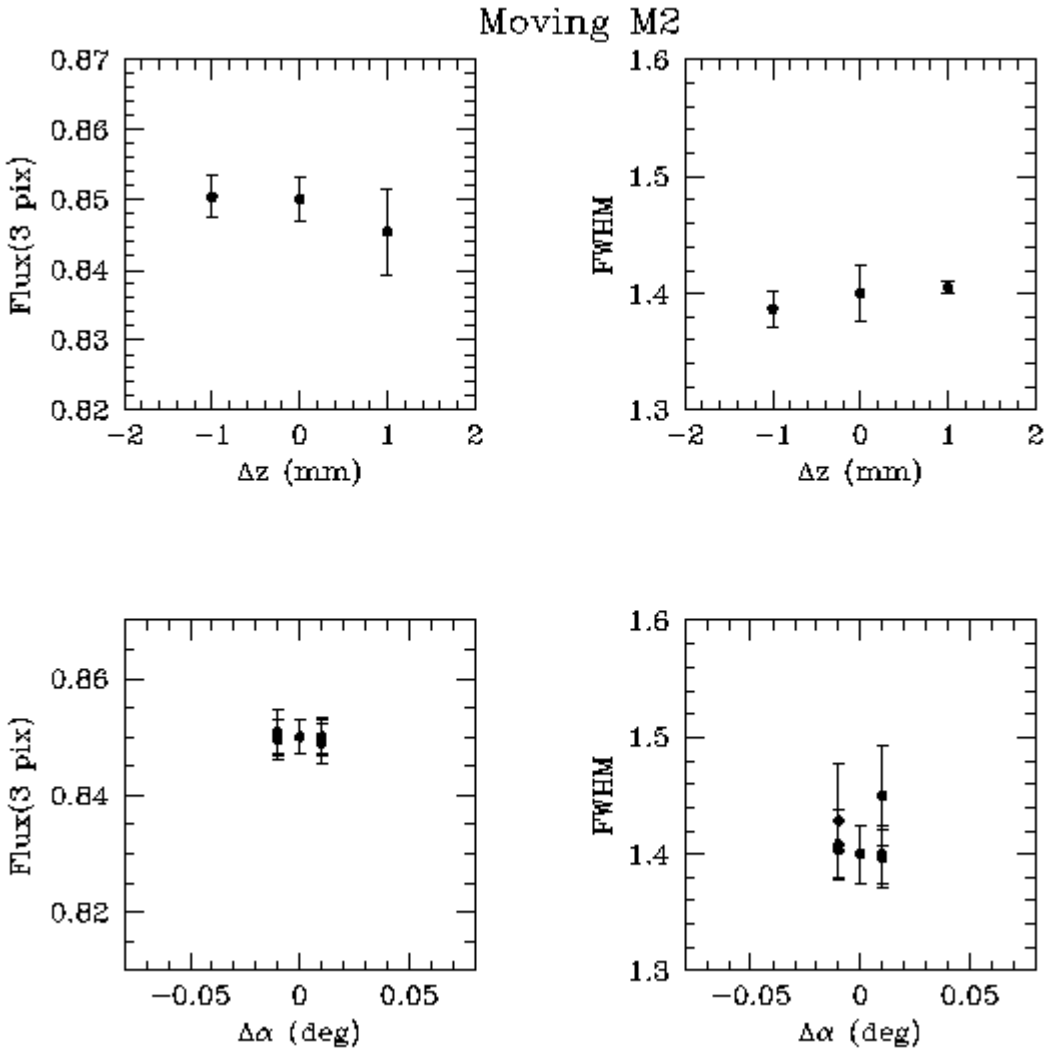

Figure 5 : changes of the encircled energy and FWHM as a function of the M2 mirror position (upper panels) and tilt (lower panels).

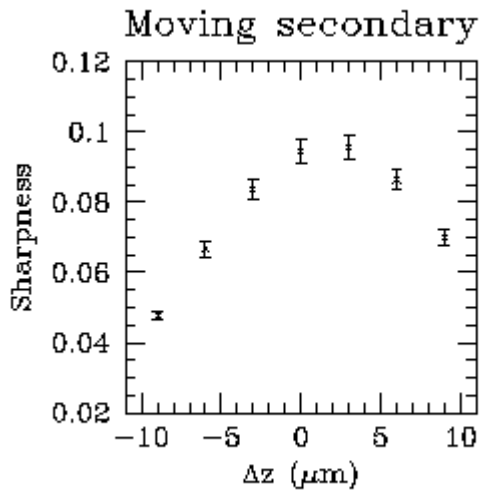

Figure 7 : changes of the PSF sharpness as a function of secondary mirror position. Notice how the error bars representing PSF position uncertainties at the subpixel level are small compared to the effect we intend to measure.

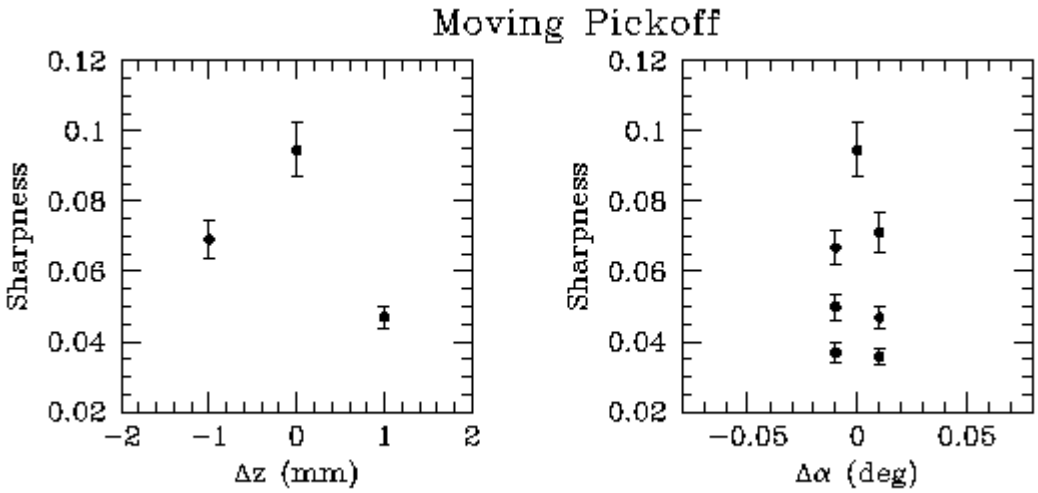

Figure 8 : changes of the PSF sharpness as a function of pickoff mirror position (left panel) and tild (right panel).

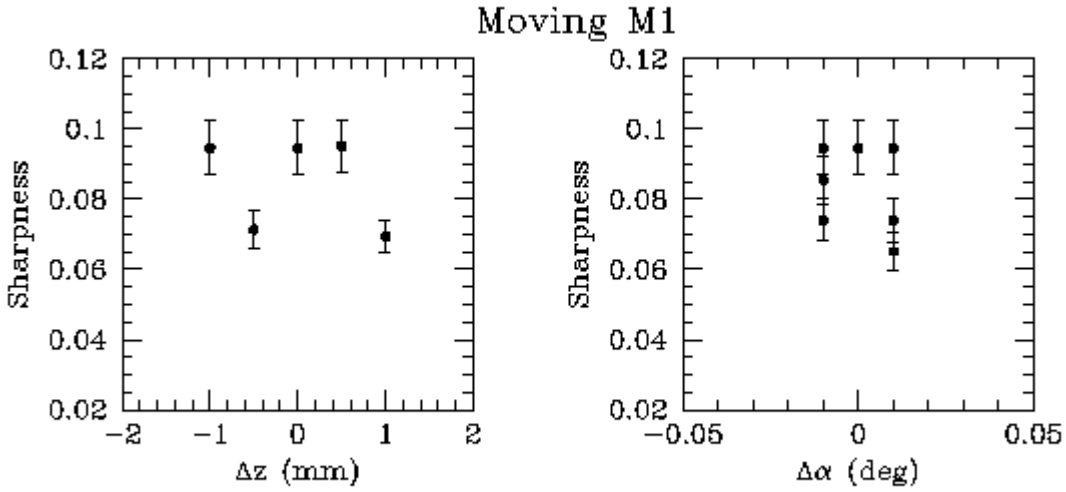

Figure 9 : changes of the PSF sharpness as a function of the M1 mirror position (left panel) and tild (right panel).

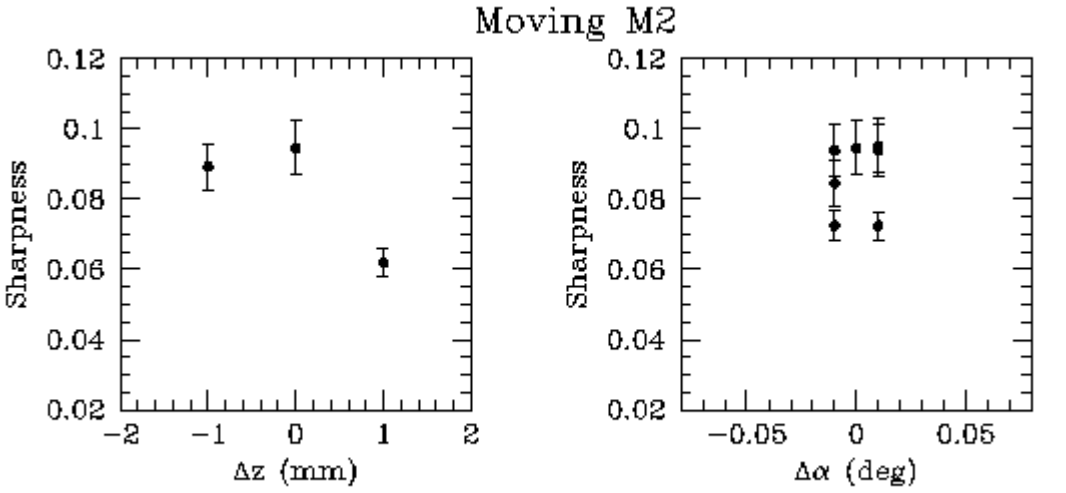

Figure 10 : changes of the PSF sharpness as a function of the M1 mirror position (left panel) and tild (right panel).

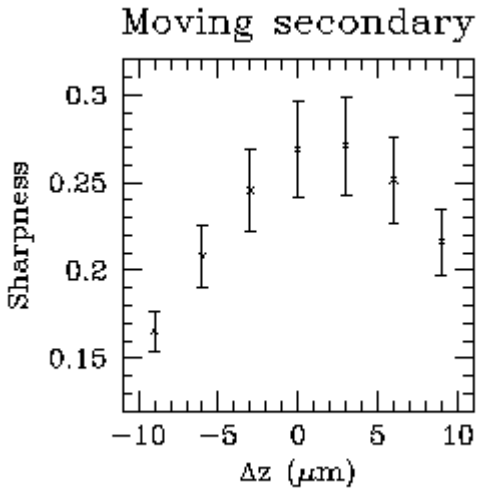

Figure 11 : changes of the PSF sharpness as a function of secondary mirror position computed for a notional instrument similar to WFC3 UVIS but with a scale on the sky similar to that of the WF chips on WFPC2.

4. Discussion

From the figures presented it is immediately apparent that encircled energy and PSF FWHM cannot be used to check the focus and alignment of WFC3 UVIS. Improving the measurement over the accuracy achieved in the present simulations would require either using many tens of stars for the measurement or calibrating and correcting for the sub-pixel position effect. Sharpness is a lot more promising as a technique even though it is still of limited applicability for some of the optical element displacements that we would need to monitor.

It is clear that the limited applicability of the sharpness technique is partly due to the (slight) undersampling of the WFC3 UVIS PSF at 630 nm. The same technique would be much more powerful for a better sampled PSF and much less sensitive to sub-pixel centering uncertainties. In order to verify this we have created PSF for a notional instrument similar to WFC3 UVIS but with the same pixel scale on the sky as the WF chips of WFPC2 (0.1 arcsec). A comparison of Figure 11 and 7 shows how this simple change of pixel size has major impact on the accuracy of the technique: for the WFC3 scale secondary mirror displacements of 3 mm are easily measurements but are below the sensitivity of the WF/WFPC2 scale. The fact that the level of undersampling determines how successful the sharpness technique can be, suggests that its performance for the WFC3 IR channel will be no better than for the UVIS channel.

5. Future plans

In the future we are planning to repeat a similar study aimed at providing guidance for the optical alignment of both WFC3 channels. The new study will remove some of the limitations of the present one by:

- Considering an improved algorithm for computing the encircled energy and exploring a range of radii. The new algorithm will be similar to that used for the alignment of ACS and will include improved sub-pixel centering treatment and partial pixel contribution. The improve algorithm and a small aperture may render the encircled energy more competitive.
- Including a noise contribution in the simulated images. It is known (e.g. Hartig, private communication) that sharpness is more sensitive to noise than, e.g., the encircled energy.
- Considering an improved algorithm for computing the PSF FWHM through sub-pixel resolution gaussian model fits. This should decrease the dependence of the measured FWHM on sub-pixel centering.
- Improve the description of the detector PRF either by using one measured for the WFC3 detectors or – should such a characterization be unavailable - using for the UVIS channel the one measured for ACS/WFC.

Acknowledgements

We thank Neill Reid and George Hartig for a careful reading of the manuscript.